Electronic Supplementary Material (ESI) for Nanoscale Horizons.

Supporting Information

Synthesis of Monodisperse High Entropy Alloy Nanocatalysts from Core@Shell Nanoparticles

Yifan Chen,[a,c] Xun Zhan,[b] Sandra L. A. Bueno,[a] Ibrahim Shafei,[a] Hannah M. Ashberry,[a] Kaustav Chatterjee,[a] Lin Xu,[c] Yawen Tang*[c] and Sara E. Skrabalak*[a]

[a]Department of Chemistry, Indiana University, 800 E. Kirkwood Ave. Bloomington, IN 47405.
*E-mail: sskrabal@indiana.edu (S. Skrabalak)
[b]Electron Microscopy Center, Indiana University, 800 E. Kirkwood Ave. Bloomington, IN 47405.
[c]Jiangsu Key Laboratory of New Power Batteries, Jiangsu Collaborative Innovation Center of Biomedical Functional Materials, School of Chemistry and Materials Science, Nanjing Normal University, Nanjing 210023, China.
*E-mail: tangyawen@njnu.edu.cn (Y. Tang)

EXPERIMENTAL SECTION

Materials and reagents. Oleylamine (70%, OLA), oleic acid (90%, OA), trioctylphosphine (97%, TOP), 1,2-dodecanediol (90%, DDD), 1-octadecene (90%, ODE), platinum bromide ($PtBr_2$), copper(II) acetate ($Cu(ac)_2$), palladium(II) bromide ($PdBr_2$), cobalt(II) acetate tetrahydrate ($Co(ac)_2 \cdot 4H_2O$), nickel acetylacetonate ($Ni(acac)_2$) and perchloric acid solution ($HClO_4$, 1.0 M) were purchased from Sigma-Aldrich and unaltered. Nafion (LQ-1105-110 EW at 5%) and Pt reference (10% Pt on carbon) were purchased from the Fuel Cell Store. Nanopure water (18.2 MΩ cm) was used for all electrochemical testing. All chemicals were used without further purification.

Synthesis of PdCu B2 Seeds: The PdCu B2 seeds were synthesized as previously described by the Skrabalak group.[1] To a 100 mL round-bottom flask were added 0.100 mmol of $Cu(ac)_2$, 0.100 mmol of $PdBr_2$, 9.0 mL of OLA, and 10 µL of OA, and this mixture was heated under vacuum to 110 °C and held for 10 min with stirring. Then, 50 µL of TOP was added, and the solution was heated to 235 °C under Ar and held at this temperature for 20 min. The solution was allowed to cool to room temperature naturally. Size selection was necessary to get sample monodispersity. The solution was transferred to a centrifuge tube along with 20 mL of hexane. The solution was spun at 3.9 rpm for 10 min to collect the particles and then the obtained particles were washed 3 times with a mixture of ethanol and hexane (5:1 vol). The particles were suspending in hexane for further use.

Synthesis of PdCu B2@PtNiCo: The PdCu seeds (6 mg) were added to a 100 mL RBF containing 17 mg of $PtBr_2$, 11.7 mg of $Ni(acac)_2$, 17.4 mg of $Co(ac)_2 \cdot 4H_2O$, 1322 mg of DDD, 7.0 mL of ODE, and 2.0 mL of OLA. This was heated to 110 °C under vacuum and held at that temperature for 10 min. The temperature was then increased to 235 °C under Ar blanket and was allowed to incubate for 25 min. The solution was allowed to cool to room temperature naturally and transferred to a centrifuge tube along with 10 mL of hexane. The solution was spun at 3.9 rpm for 10 min to remove the larger particles. Then, the rest of the particles were precipitated out by acetone and collected by centrifugation at 11K rpm for 10 min. The particles were washed 3 times with a mixture of ethanol and hexane (5:1 vol). The particles were suspending in hexane for further use.

Synthesis of PdCuPtNiCo HEAs/C: As-synthesized PdCu B2@PtNiCo NPs were evenly dispersed on a carbon support (Ketjen EC-600JD). The NPs were massed and then resuspended in 1 mL of hexane. The NPs were then added dropwise to a slurry of the carbon support in 5 mL acetone and 2.5 mL hexane. The mass ratio between the NPs and carbon support was 1:9. Once the NPs were added, the solution was sonicated for 1 h and then left to stir overnight. The solvents were then evaporated, and the resulting catalyst dried in vacuum overnight. The obtained solids were dissolved in acetone solution by sonicating and transferred onto a quartz crucible to let it dry naturally. The boat was centered in a fused silica tube and heated in a tube furnace. The fused silica tube was purged with a H_2/N_2 (4 v/v%) mixture for 30 min, and then the sample was heated to 600 °C for 10 h at a ramp rate of 20 °C min^{-1}.

One-Step Synthesis of PdCu@PtNiCo NPs: To a 100 mL round-bottom flask were added 18 mg of $Cu(ac)_2$, 36 mg of $PdBr_2$, 17 mg of $PtBr_2$, 11.7 mg of $Ni(acac)_2$, 17.4 mg of $Co(ac)_2 \cdot 4H_2O$, 1322 mg of DDD, 7.0 mL of ODE, and 2.0 mL of OLA. This was heated to 110 °C under vacuum and held at that temperature for 10 min. The temperature was then increased to 235 °C under Ar and was allowed to incubate for 25 min. The particles were cooled and collected as previously described in the synthesis of PdCu B2 Seeds.

Characterizations. All NPs were characterized on JEOL JEM 1010 TEM, which operated at 80 keV. TEM samples were drop-cast onto the carbon-coated Cu grids after the entire sample was washed two to three times as described below. Additional characterization with STEM-EDS was completed with JEOL JEM 3200FS operating at 300 keV and a JEOL 2200FS operating at 200 keV. The TEM samples were prepared as described above, but carbon-coated Au grids were used. Atomic resolution HAADF STEM imaging was conducted using the Thermo Scientific Themis Z operating at 300 keV. To obtain high quality STEM images, nanoparticles should be collected after reaction as soon as possible, and washed 6-9 times using mixture of ethanol and hexane (5:1 vol) to remove excess capping agents. SEM-EDS was performed with a FEI Quanta 600F Environmental SEM operating at 30 kV. The power diffraction (XRD) was collected on a PANalytical Empyrean instrument with Cu Kα radiation and an X'Celerator linear strip detector. X-ray photoelectron spectroscopy (XPS) was performed on a PHI 5000 VersaProbeTM II instrument equipped with a focused monochromatic Al Kα source. A beam size of about 100 μm and an X-ray power of 50 W at 15 keV under ultra-high vacuum (UHV) conditions was used for all experiments. The binding energy was calibrated using C 1s peak at 284.8 eV.

Electrochemical Measurements: A Pine Rotating disk electrode (RDE) was used to collect ORR measurements, with AfterMath 1.3.7060 software. A typical three-electrode cell was used where the working electrode was glassy carbon (0.238 cm^2), the reference electrode was Ag/AgCl (4 M KCl), and a graphite rod was used as the counter electrode. The working electrode was prepared by creating a 5 mg mL^{-1} ink solution of the catalysts, where the solution consisted of 1:3.98:0.020 volumetric ratio of isopropanol:H_2O:Nafion. The catalyst ink was sonicated for 30 min and 10 μL was dropcast onto the glassy carbon electrode and dried. The Pt loading was determined by using the metal ratios determined by SEM-EDS in combination with the catalyst preparation method (a 9:1 mass ratio of carbon support to nanocatalyst).

Normalization of the electrode by sweeping 200 times between 60 mV and 1200 mV *vs.* reversible hydrogen electrode (RHE) was performed first to remove any excess surfactant or surface contamination. Hydrogen desorption experiment were used to determine the electrochemically active surface area (ECSA) and were performed by cycling between 60 and 1000 mV *vs.* RHE in an Ar purged 0.1 M $HClO_4$ solution. The area under the hydrogen desorption peaks was measured and converted to the active surface area, assuming 210 μC cm^{-2} for the adsorption of a hydrogen monolayer on a polycrystalline Pt surface. The value obtained was then normalized by the Pt loading on the electrode.

The ORR activities of the catalysts were measured via the RRDE voltammograms in a 0.1 M KOH electrolyte at a rotation rate of 1600 rpm and a scan rate of 10 mV s^{-1}. Before testing, O_2 was purged into the electrolyte for at least 30 min to saturate the electrolyte with O_2. Accelerated durability testing was collected by cycling between 0.6 and 1.0 V *vs.* RHE in O_2-purged 0.1 M KOH 10000 times. All potentials in this work have been calibrated into the RHE. The percentage of peroxide species (HO_2^-%) and electron transfer number (n) are calculated by the following equations[2]:

$$\mathrm{HO_2^-}\% = \frac{200 I_r}{N I_d + I_r} \qquad n = \frac{4 N I_d}{N I_d + I_r}$$

where I_d is the disk current, I_r is the ring current, and N is the current collection efficiency of the Pt ring, which is determined to be 0.37.

Lattice Mismatch Calculation: the following equations was used to calculate the lattice mismatch using the d-spacing of the planes comprising the interface of the B2 and shell materials.

$$\%\boldsymbol{diff} = \frac{\boldsymbol{d_{B2} - d_{shell}}}{\frac{\mathbf{1}}{\mathbf{2}}(\boldsymbol{d_{B2} + d_{shell}})} \times \mathbf{100}$$

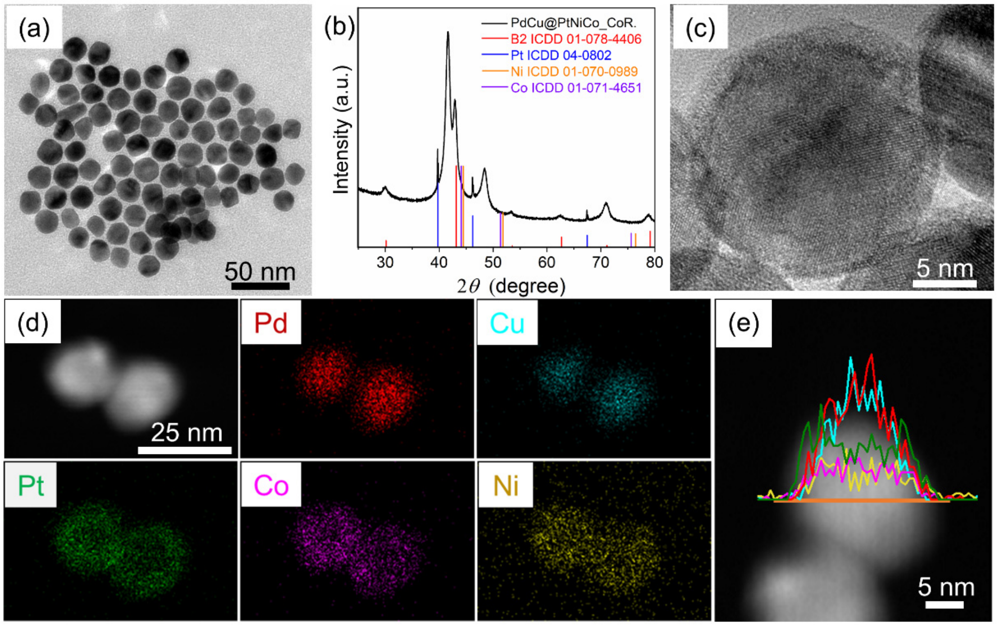

Fig. S1. Morphological and compositional characterization of PdCu@PtNiCo NPs from one-step synthesis: (a) TEM bright-field image, (b) XRD pattern, (c) HRTEM image, (d) STEM-EDS elemental mapping images, and (e) line scan profile.

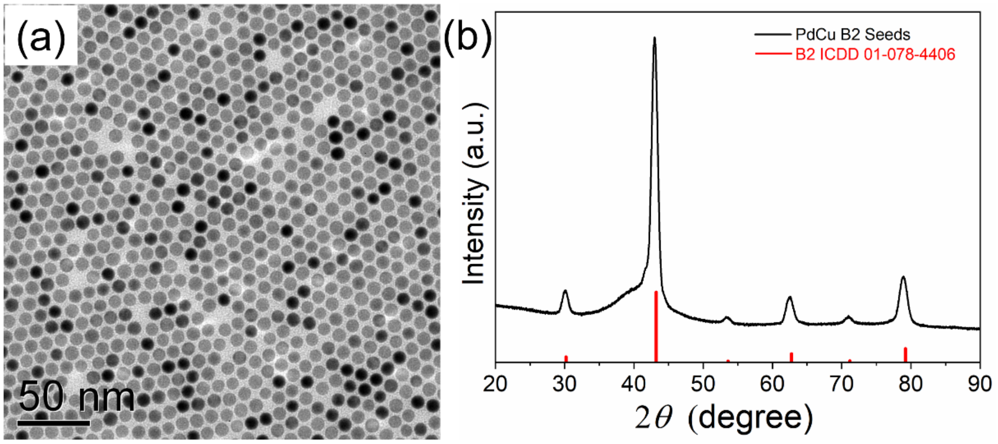

Fig. S2. (a) TEM bright field image and (b) XRD pattern of PdCu B2 seeds.

Table S1. Summary of the atomic composition determined by SEM-EDS. The EDS measures are ensemble measurements.

Atomic %	Pd	Cu	Pt	Ni	Co
PdCu B2@PtNiCo	20	17	22	21	20

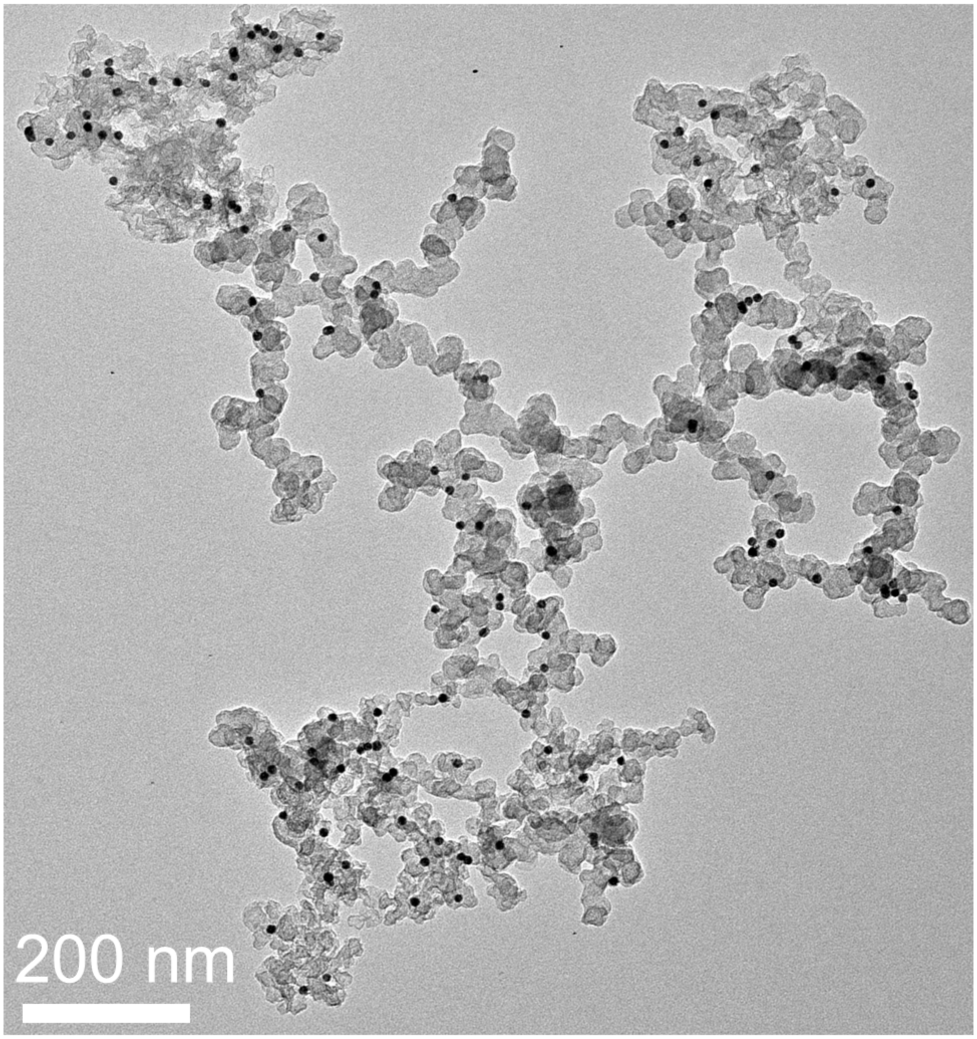

Fig. S3. TEM bright-field image of PdCu B2@PtNiCo/C.

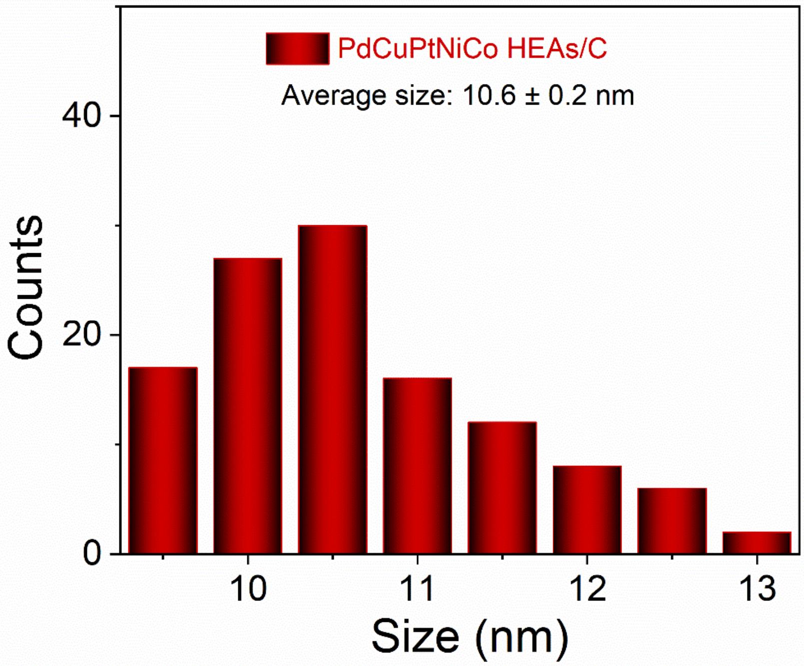

Fig. S4. Size distribution of the synthesized PdCuPtNiCo HEAs/C.

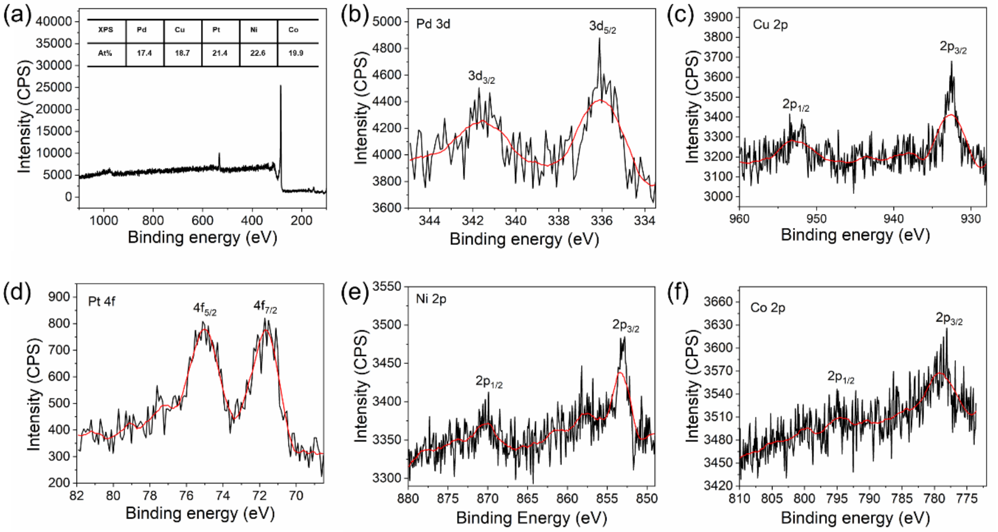

XPS	Pd	Cu	Pt	Ni	Co
At%	17.4	18.7	21.4	22.6	19.9

Fig. S5. XPS spectra (a) survey scan and (b) Pd 3d, (c) Cu 2p, (d) Pt 4f, (e) Ni 2p, and (f) Co 2p regions of the PdCuPtNiCo HEAs/C. The low signals are due to the low loading of NPs compared to carbon support.

Table S2. (a) Summary of the d-a relationship of different facets in random alloy FCC, Fm$\bar{3}$m, ordered CsCl-like, Pm$\bar{3}$m, and ordered BCC, Im$\bar{3}$m structure. (b) The θ value obtained from the XRD pattern of PdCuPtNiCo HEAs/C. (c) Summary of the sinθ relationship and their corresponding structure based on Bragg's Law: $2d\sin\theta=n\lambda$.

(a)	Random alloy FCC, Fm$\bar{3}$m		Ordered CsCl-like, Pm$\bar{3}$m		Ordered BCC, Im$\bar{3}$m	
	Facet	d-a relationship	Facet	d-a relationship	Facet	d-a relationship
	{111}	$d1=a/\sqrt{3}$	{100}	$d1=a$	{110}	$d1=a/\sqrt{2}$
	{200}	$d2=a/2$	{110}	$d2=a/\sqrt{2}$	{200}	$d2=a/2$
	{220}	$d3=a/2\sqrt{2}$	{111}	$d3=a/\sqrt{3}$	{211}	$d3=a/\sqrt{6}$

(b)	PdCuPtNiCo HEAs/C	$\theta1=41.5^{\circ}/2$	$\theta2=48.3^{\circ}/2$	$\theta3=70.6^{\circ}/2$
(c)	PdCuPtNiCo HEAs/C	Calculation	Approximate value	Corresponding structure
	Sinθ2/Sinθ1	1.1554	$2/\sqrt{3}$	d2/d1 in FCC
	Sinθ3/Sinθ2	1.4133	$\sqrt{2}$	d3/d2 in FCC
	Sinθ3/Sinθ1	1.6335	$2\sqrt{2}/\sqrt{3}$	d3/d1 in FCC

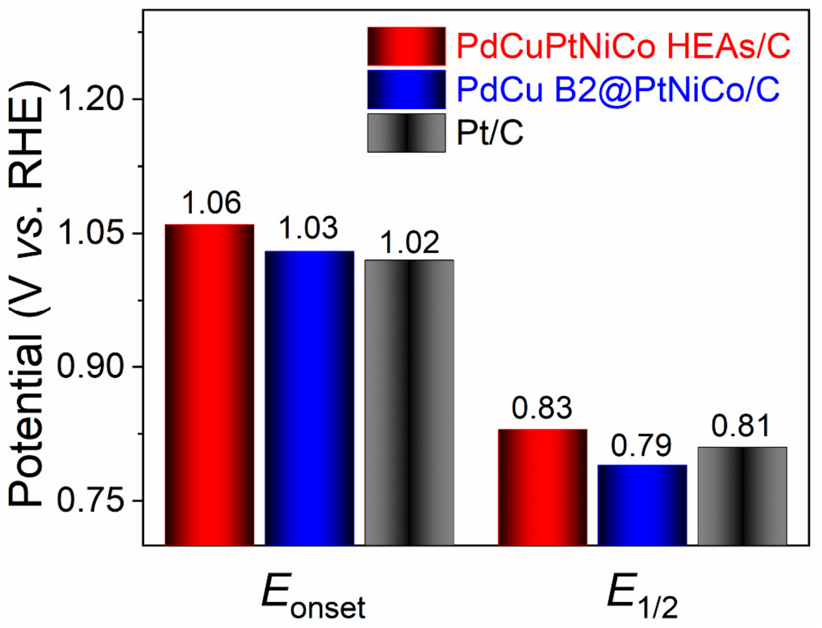

Fig. S6. Evaluation of ORR performance of PdCuPtNiCo HEAs/C, PdCu B2@PtNiCo/C, and Pt/C: E_{onset} and $E_{1/2}$ comparison.

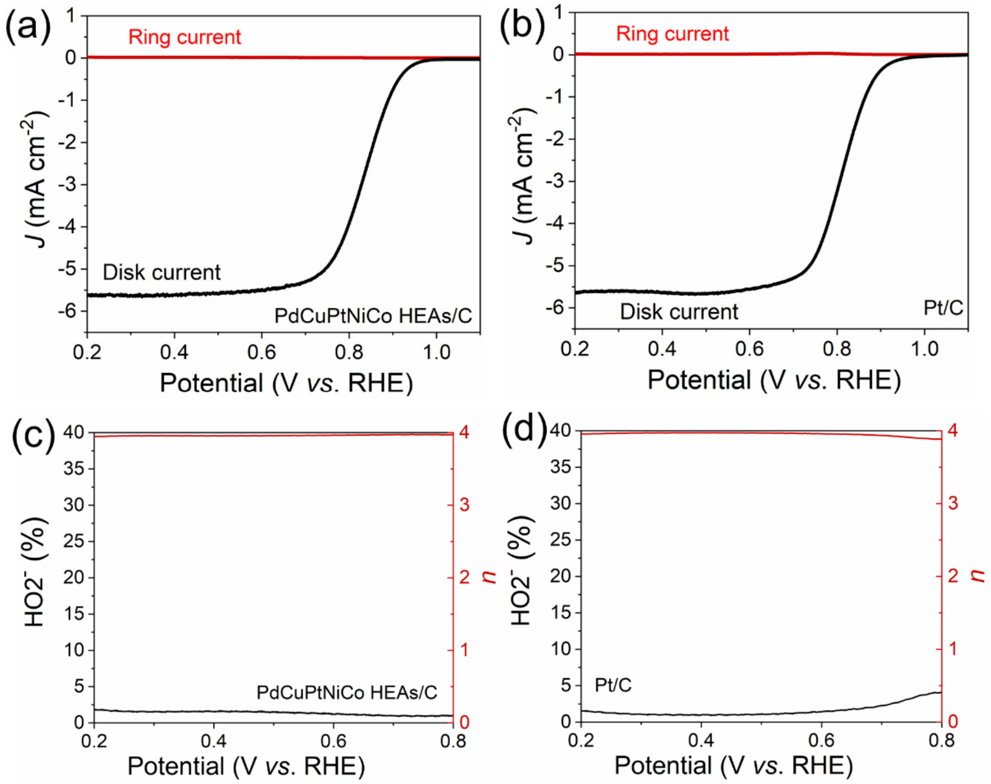

Fig. S7. RRDE test of (a) PdCuPtNiCo HEAs/C and (b) Pt/C. The HO_2^- yield and *n* of (c) PdCuPtNiCo HEAs/C and (d) Pt/C.

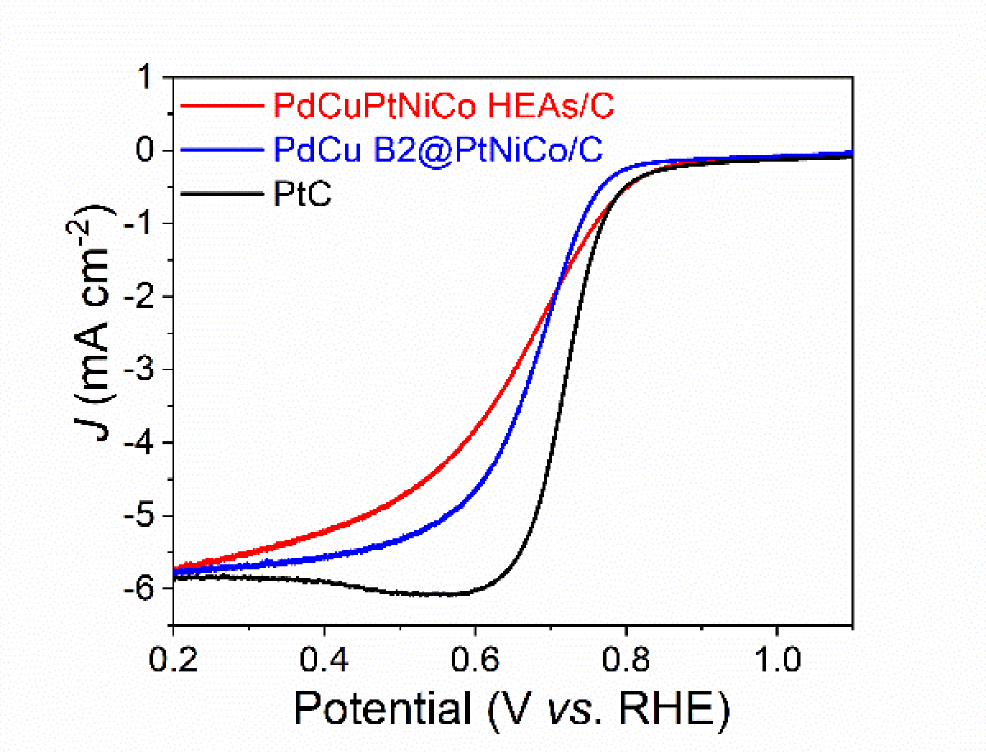

Fig. S8. Evaluation of ORR performance of PdCuPtNiCo HEAs/C, PdCu B2@PtNiCo/C, and Pt/C: LSV curves recorded in O_2-saturated 0.1 M $HClO_4$ solution with a rotation rate of 1600 rpm.

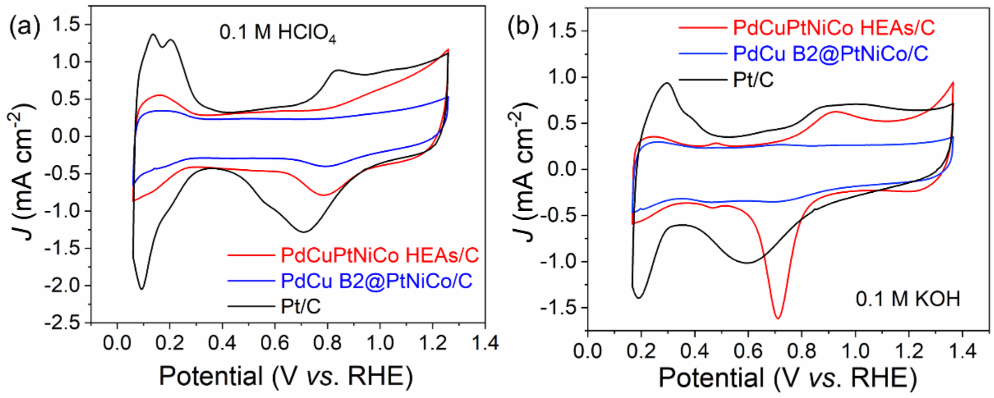

Fig. S9. Cyclic voltammograms of PdCuPtNiCo HEAs/C, PdCu B2@PtNiCo/C, and Pt/C collected in Ar-purged (a) 0.1 M $HClO_4$ and (b) 0.1 M KOH.

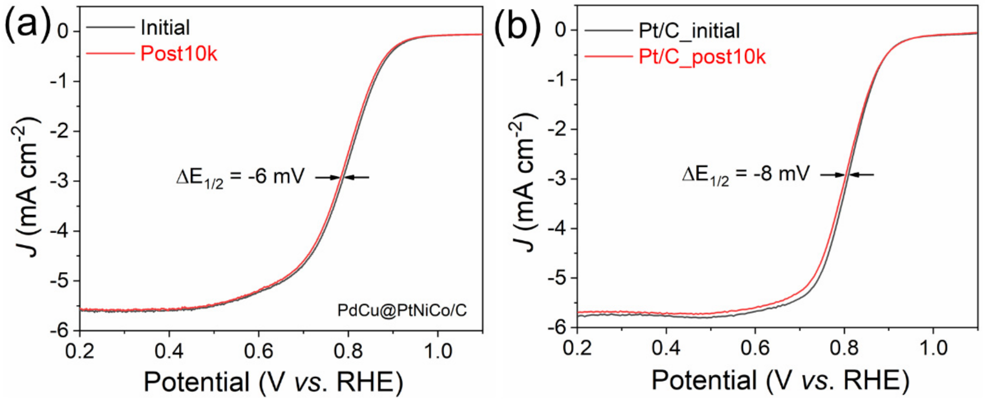

Fig. S10. ORR polarization curves of (a) PdCu B2@PtNiCo/C and (b) Pt/C before and after 10000 cycles.

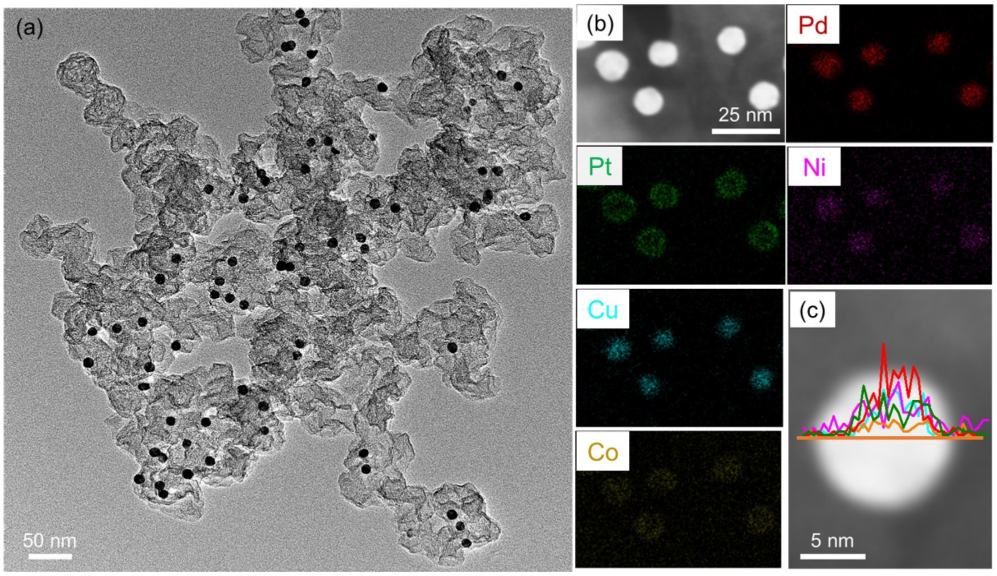

Fig. S11. (a) TEM bright-field image, (b) STEM-EDS elemental mapping images, and (c) line scan profile of PdCuPtNiCo HEAs/C after ADT.

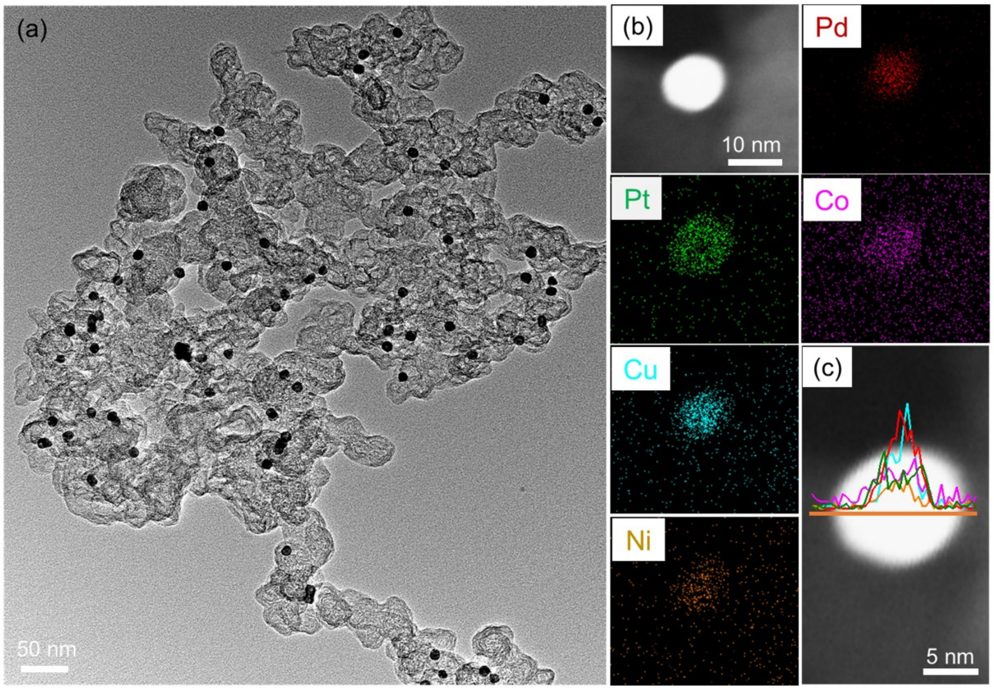

Fig. S12. (a) TEM bright-field image, (b) STEM-EDS elemental mapping images, and (c) line scan profile of PdCu B2@PtNiCo/C after ADT.

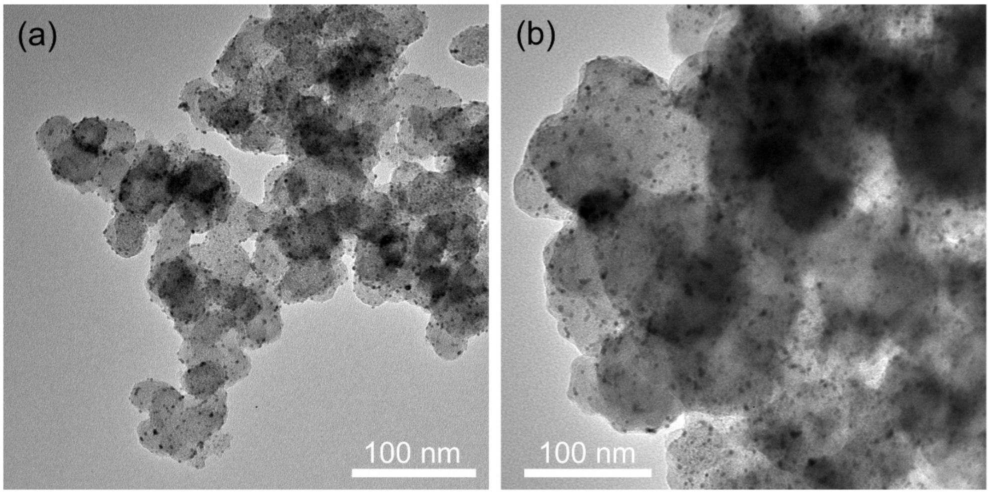

Fig. S13. TEM bright-field images of the Pt/C (a) before and (b) after ADT.

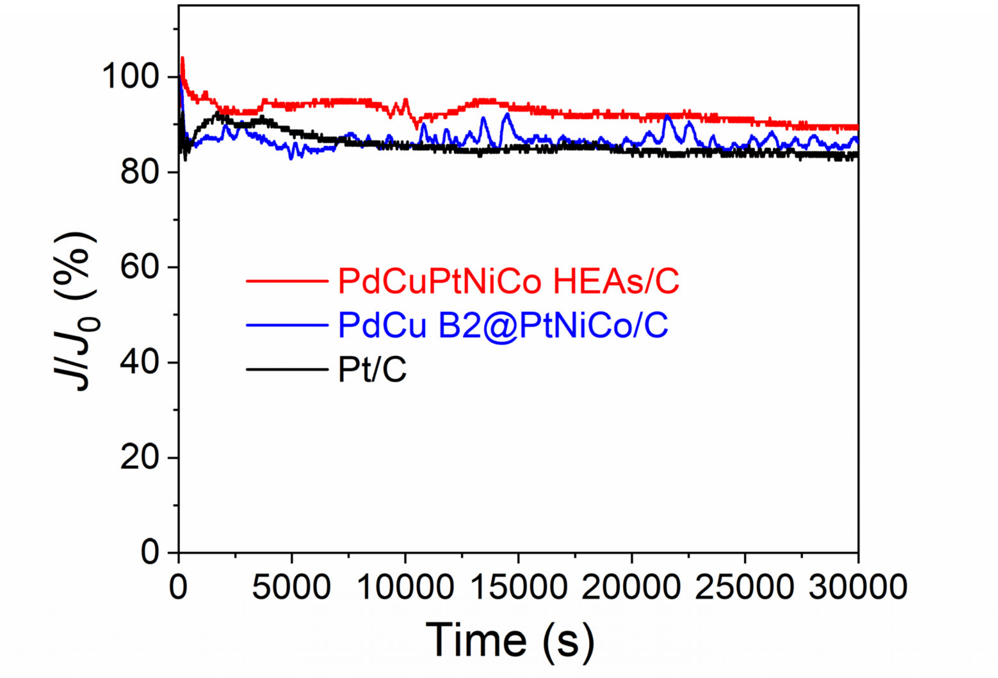

Fig. S14. Evaluation of ORR performance of PdCuPtNiCo HEAs/C, PdCu B2@PtNiCo/C, and Pt/C: relative i-t curves at 0.7 V.